

THE PERFORMANCE OF THE CUTTING HEAD OF THE LONGITUDINAL SHAFT ANCHOR EXCAVATION MACHINE BASED ON THE FUZZY NUMBER AND ENTROPY EVALUATION METHOD

Zhengqi ZHANG, Zongming ZHU*

Shuo QIAO, Daiyong LIN

¹ College of Mechanical & Electrical Engineering, Changsha University, Changsha, Hunan 410022, China

Abstract: The longitudinal shaft anchor excavation machine is a new type of excavating machinery; the cutting head directly participates in cutting work. This paper focuses on the performance parameters of the cutting head. Two variables of the cutting head are selected to study, that is, the included the alloy head clip angle and the alloy head diameter. The installation angle of the pick is 55° and the section spacing is 60 mm. Three groups of data were selected for each variable, and the ANSYS finite element analysis software was used to simulate the rock cutting of the pick, and the load characteristics of the pick were obtained. The fuzzy number principle and entropy evaluation method are used to evaluate the load fluctuation, specific energy consumption, and pick load of three groups of data in each variable, and then the optimal performance parameters of the pick are obtained. The specific work is as follows: 1. Two parameter variables of the pick are selected and analyzed by LS-DYNA simulation software to obtain the cutting load of the pick at work. 2. Determine the index set and evaluation set of the cutting head, use the fuzzy number principle and entropy evaluation method to calculate the weight of each parameter variable, create the fuzzy number relation evaluation matrix of performance parameters, and then use the fuzzy number comprehensive evaluation model to calculate the fuzzy number comprehensive evaluation result vector, finally get a set of optimal performance parameters of the pick. The final results show that the cutting head has the best performance when the alloy head clip angle is 100° and the alloy head diameter is 11 mm.

Keywords: *fuzzy number principle, entropy evaluation method, pick, pick arrangement, cutting force analysis*

* Corresponding author: 330564704@qq.com (Z. Zhang)

1. INTRODUCTION

The cutting head is the most important and key part of the longitudinal shaft anchor excavation machine in the excavation of the mine cross-section. In the whole section excavation process, the cutting head is directly involved in coal rock crushing, the efficiency of mine excavation has a great relationship with it, its role is mainly used to cut coal rock (Su, Akkaş 2020). In the actual working process, 65–85% of the power consumption in the cutting head, and the cutting head work stability directly affect the load, efficiency, specific energy consumption, and dust production is the key factor in determining the machine's performance. In order to further improve the quality of the pick, prolong the service life of the pick, and make it better able to apply to the operation condition of the rock hardness is higher (Eshaghian et al. 2021). Under the same conditions of pick material, cemented carbide properties, brazing quality, pick installation angle, and section spacing, the influence of alloy head clip angle and alloy head diameter on pick performance were studied (Qiao et al. 2021).

In recent years, scholars of various countries have done more in-depth research on the design and improvement of the longitudinal shaft anchor excavation machine cutting head. In particular, a lot of analysis and research has been done on the performance of cutting head, and a large number of scientific research achievements have been summarized, which lays a foundation for the further research of later scholars. Researchers at home and abroad have conducted a series of research and exploration on the performance of the cutting head through traditional theoretical analysis methods and based on finite element method and discrete element method. Here's the latest research: Yixue Li used ANSYS Workbench to study the connection between cutting head structure and load under the same temperature field and different rock conditions and found that the strain changes of pick, pick seat posit, and the cutting head was in a reasonable and affordable range (Yixue 2019). Wang uses ADAMS to analyze the mapping relationship between vibration signals of cutting head and rock hardness and carries out dynamic analysis on the cutting mechanism of the excavation machine under different parameters (Wang 2020). Osman Zeki Hekimoglu has carried out a full-scale simulation of cutting heads of various practical types of excavation machines with various inclination angles through laboratory straight-line cutting experiments. The experiments show that it is not recommended to use more than the optimal inclination angle for measuring tools and angle picks (Hekimoglu 2018). However, through a large number of experiments, it is found that most scholars keep a single variable for the performance evaluation of the cutting head, which often requires a large number of experiments. In this way, we may find that there are different optimal parameters under different conditions. Often, when one index is excellent, another index cannot meet our requirements, so we cannot evaluate whether the overall performance of the cutting head is excellent. At this time, we need to introduce the

fuzzy number and entropy evaluation method to do an overall evaluation of the cutting head, to judge whether the performance of the cutting head is good enough under this condition.

2. MODEL ESTABLISHMENT AND PARAMETER SETTING STEPS

2.1. SELECTION OF ROCK MATERIAL CONSTITUTIVE MODEL

The Holmquist–Johnson–Cook model is adopted in this paper (Holmquist et al. 1993). This model is a material damage model proposed by Holmquist et al. The constitutive model is mainly used to solve the large deformation problems of rocks and other materials. It mainly focuses on the evolution of compression damage of materials and considers the pressure dependence of compression strength, strain rate effect, and damage softening effect. Its equivalent yield strength is a function of pressure, strain rate, and damage, while pressure is a function of volume strain, and damage accumulation is a function of plastic volume strain, equivalent plastic strain, and pressure. The model is mainly composed of three equations, namely yield surface equation, compression state equation, and damage evolution equation.

The yield surface equation (Wu et al. 2010) is calculated as follows:

$$\sigma^* = [A(1 - D) + BP^{*N}](1 + C \ln \varepsilon^*), \quad (1)$$

where: σ^* and P^* are the dimensionless equivalent stress and hydrostatic pressure obtained by dividing the actual equivalent stress and hydrostatic pressure, respectively, by the static compressive strength f_c' of the material, ε^* is the dimensionless strain rate obtained by dividing the real strain rate by the reference strain rate ε_0 , D is the degree of injury, A , B , N , and C are the strength parameters of the material.

The damage evolution equation (Su et al. 2020) is calculated as follows:

$$D = \sum \frac{\Delta \varepsilon_p + \Delta \mu_p}{\varepsilon_p^f + \mu_p^f}, \quad (2)$$

where: $\Delta \varepsilon_p$ and $\Delta \mu_p$ are equivalent plastic strains and plastic volumetric strains in a calculation cycle, respectively, ε_p^f and μ_p^f are the equivalent plastic strain and plastic volumetric strain of crushing under normal pressure, respectively.

The element failure criterion in the Holmquist–Johnson–Cook model is based on the custom strain failure criterion (Li 2009). When the trial stress of a certain element

in the rock exceeds its strength, plastic deformation will occur. When the plastic strain accumulates to the defined failure strain, LS-DYNA can delete this element by using erosion algorithm.

2.2. DETERMINE THE PARAMETERS OF THE HOLMQUIST-JOHNSON-COOK MODEL KEYWORD

In the LS-DYNA display dynamics analysis program, material parameters can be assigned to the finite element model by the Holmquist–Johnson–Cook model keyword file. The keywords of the Holmquist–Johnson–Cook model are shown in Fig. 1. In the figure, MID is the material number assigned by the parameter, ρ is the material density (represented by RO in the figure), G is the material shear modulus, and ESPO is the material reference strain rate (Qiao et al. 2022).

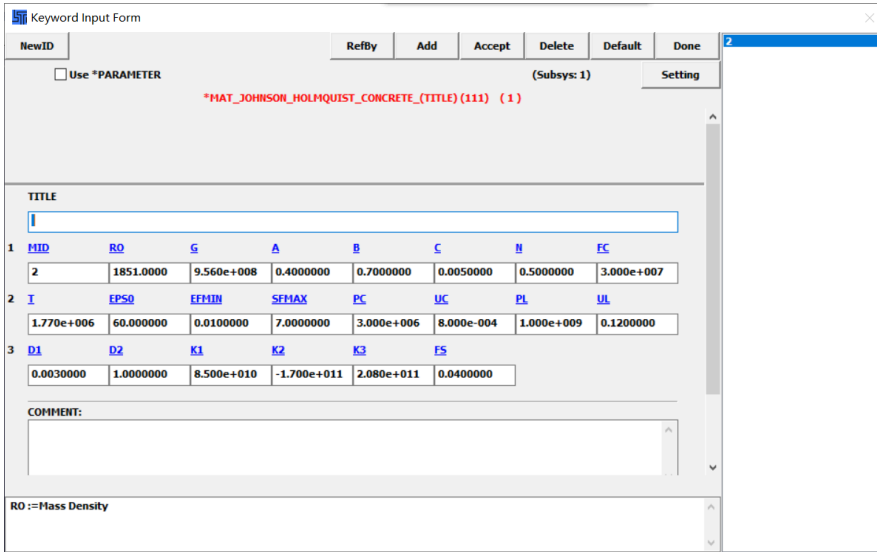


Fig. 1. The Holmquist–Johnson–Cook model parameter definition

2.3. ESTABLISHING FINITE ELEMENT MODEL

2.3.1. CUTTING ANGLE

This step carries on the model establishment and the parameter setting. Use Solid-Works software to establish the three-dimensional model of the pick, pick seat posit, rotating support, and rock, and then merge the pick, pick seat posit, rotating support, and rock into the assembly, save the assembly as x.t file, and export. In this paper, the internal stress of the pick is not analyzed. In order to facilitate the establishment of the

simulation model and speed up the subsequent solving speed, the complex internal structure is omitted in the establishment of the 3D model, and the same shape of the 3D pick and tooth seat is adopted. The installation angle is 55° , as shown in Fig. 2 (Qiao et al. 2021).

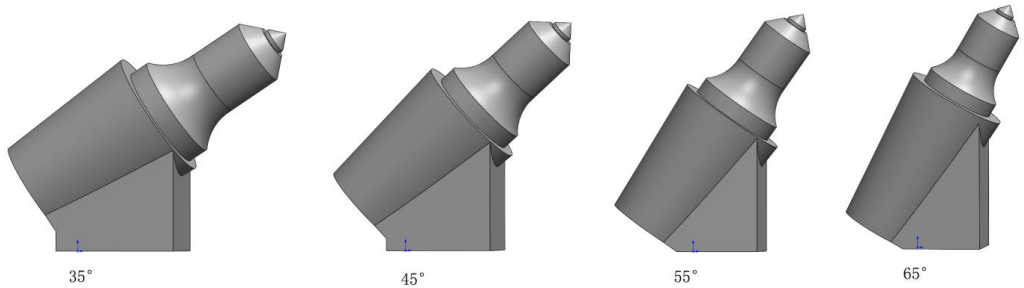


Fig. 1. Cutting angle of picks

2.3.2. SECTION SPACING

Section spacing is the distance between two adjacent picks on the axis direction of the rotating support. If the section spacing is too small, the distribution of the pick is too dense, the dust production will increase in the cutting head, the energy utilization rate is low, and the work efficiency becomes low. Conversely, when the section spacing is too large, the resistance on each of the picks will be high (Qiao et al. 2021).

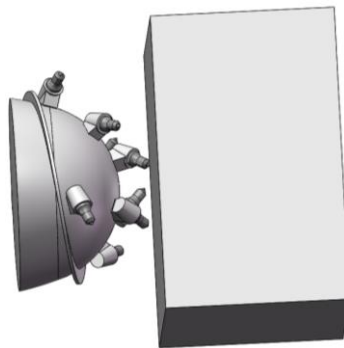


Fig. 3. Cutting head model

In this paper, a cutting head with a section spacing of 60 mm was selected. During the simulation, the simplified model of a partial cutting head can be used to analyze the influence of different section spacing on cutting performance. The cutting head model

is shown in Fig. 3.

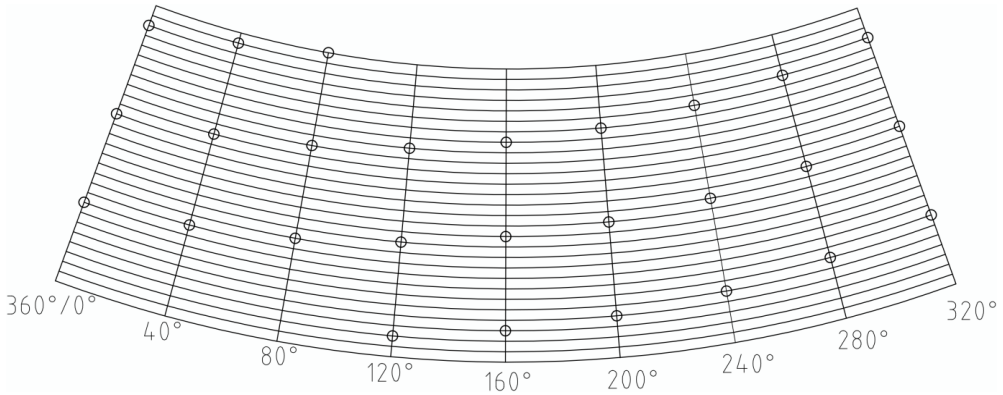


Fig. 4. Lateral expansion of pick arrangement

2.3.3 SPIRAL LINE OF PICK

When the excavation machine is working, the cutting head produces cutting force on the rock, so as to achieve the effect of cutting. In general, the picks on the cutting head are arranged in a spiral pattern that makes it easier for the rock to be removed. A large number of studies have shown that the number of spiral lines will affect the cutting effect of the cutting head.

A single helix line design is adopted in this paper. A single helix line can make the cutting head structure simple, ensure the arrangement of the pick, and reduce the actual installation workload and installation difficulty of the pick. But because the single helix line cutting head is cut more finely, they produce more dust (Zhang, Zhang 2020).

The spiral angle of the pick also affects the design of the cutting head. If the spiral angle of the pick is too small, it will increase the density and number of the pick and increase the weight of the cutting head at the same height. When the spiral angle of the pick is too large, for the same height of the cutting head, it will reduce the density and number of the pick, increasing the loss of the pick, which is not conducive to the cost performance. The spiral angle of the pick adopted in this paper is 6° .

For the pick on the cutting head, the motion speed of the pick can be decomposed into three motion vectors v_x , v_y , v_z . Figure 5 is the spiral line schematic diagram.

It can be seen from Fig. 5 that the spiral rising angle β and the three velocity vectors can be related as follows:

$$\tan \beta = \frac{|\vec{v}_z + \vec{v}_r|}{|\vec{v}|} \quad (3)$$

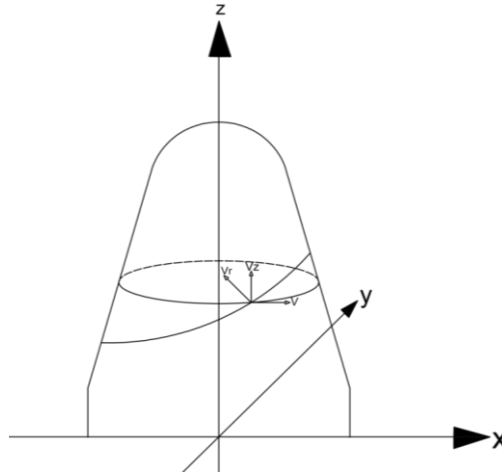


Fig. 5. Schematic diagram of spiral line

2.3.4. BUILDING A 3D MODEL

Because ANSYS/LS-DYNA could not establish the model accurately, Solid Works was used to establish the model (Stolarski et al. 2018). Pick, pick seat posit, rotating support and coal rock 3D solid model are drawn, respectively. Finally, save the x.t format for easy opening in ANSYS software.

2.3.5. MESHING STEPS

When meshing in LS-DYNA software, the rationality of the grid should be considered, and the accuracy can be selected according to the actual situation. Too large a grid

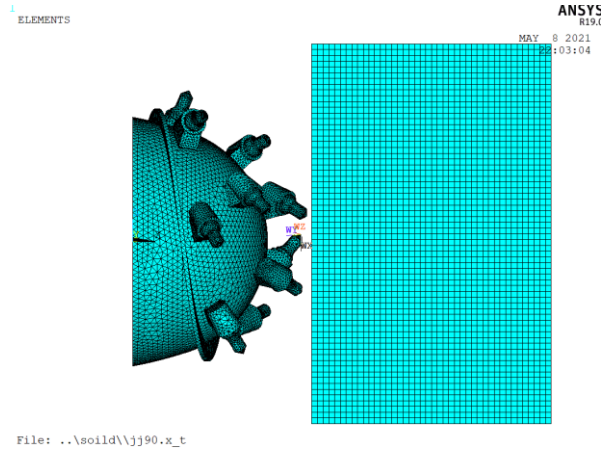


Fig. 6. Cutting head and coal rock model mesh division

may lead to negative volume, but too small a grid will lead to longer simulation analysis time. In order to balance the relationship between the two, high precision can be set in the section of pick, and low precision can be set in the section of pick seat posit, rotating support, and coal rock. However, when dividing the coal and rock mesh, the precision cannot be too low, too low precision will make the coal and rock fall off in a large area during the work of the pick, and cannot achieve the ideal result. The meshing effect is shown in Fig. 6.

2.4. PICK AND ROCK MATERIAL PROPERTIES DEFINED

The material properties are defined. The density of the rock is set as 2670 kg/m^3 , the density of the conical pick is set as 7800 kg/m^3 , the Poisson's ratio of the rock and the conical pick is set as 0.3, the shear modulus of the rock is set as 1080 MPa, the compressive strength of the rock is set as 123 MPa, and the tensile strength of the rock is set as 5.16 MPa.

Table 1. Material parameter

Parts	Density [Kg/m ³]	Poisson ratio	Shear modulus [M/Pa]	Compressive strength [M/Pa]	Tensile strength [M/Pa]
Rock	2670	0.3	1080	123	5.16
Conical pick	7800	0.3	—	—	—

2.5. CONTACT SETTINGS

When the cutting head cut coal and rock, the process of coal and rock falling off is

a dynamic process, which can be regarded as the contact problem between the rigid body and soft body. So ESTS were selected for this simulation. In LS-DYNA, we can use the keyword *CONTACT_SURFACE_TO_SURF_ERODING to achieve the desired effect.

2.6. BOUNDARY CONDITIONS AND CONSTRAINT SETTINGS

The simulation of this paper is to simulate the process of rock crushing by cutting head in the roadway because underground coal and rock have forces in all directions. Therefore, in order to prevent the simulation results from being affected, it is necessary to set reflective boundary conditions and constraints. The non-reflective boundary is established on the five sides of the rock model to make the rock fall from the other side when cutting, which is in line with the actual working state.

3. DATA PROCESSING AND ANALYSIS

3.1. THE ALLOY HEAD CLIP ANGLE

In this paper, four kinds of picks with alloy head angle of 70°, 80°, 90°, and 100° are designed. Its parameters are shown in Table 2. In order to avoid the interference caused by other factors during the simulation, the control variable method was used to set other parameters as the same, and the speed of the cutting head was set as 38 r/min.

Table 2. Structural parameters of the pick with different alloy head clip angle

Species	Alloy head clip angle [°]	Alloy head diameter [mm]	Picks shank diameter [mm]	Picks shank height [mm]
1	70	13	34	66
2	80	13	34	66
3	90	13	34	66

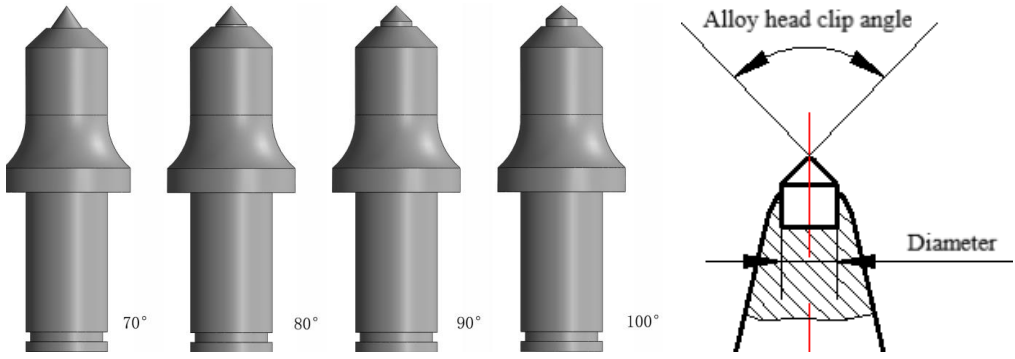


Fig. 7. Alloy head clip angle

The simulation results can obtain the total load F_W and the load F_X , F_Y , and F_Z on the X , Y , and Z axes, respectively. According to the data obtained at each point of the three-way load, the lateral load F_1 , traction load F_2 , and cutting load F_3 can be obtained, and the cutting torque, specific energy consumption, and load fluctuation can be obtained. This paper focuses on cutting load and traction load.

Let the rotation angle of the drum be β , then the cutting load F_3 is:

$$F_3 = F_Y \cos \beta + F_Z \sin \beta. \quad (4)$$

Traction resistance F_2 is:

$$F_2 = F_Y \sin \beta + F_Z \cos \beta. \quad (5)$$

Load standard deviation is used to indicate load fluctuation:

$$\sigma = \sqrt{\frac{1}{N} \sum_{i=1}^N (X_i - \mu)^2}, \quad (6)$$

where: σ is the load standard deviation, N is the number of experimental data sets, M is the average cutting force, KN.

Through simulation results and formula calculation, the average cutting force of cutting head cutting rock can be obtained when the included the alloy head clip angle is different, as shown in Table 3.

Table 3. The calculation results

Alloy head clip angle [°]	Cutting force [KN]	Traction [KN]	Resultant force [KN]	The standard deviation of the resultant force	Torque [KN*m]
70	2.41	2.73	3592.64	261.33	77.99
80	26.54	12.99	3533.97	227.22	68.09

90	20.64	-24.54	3561.44	233.43	67.98
100	36.89	-1.20	3589.53	228.36	63.80

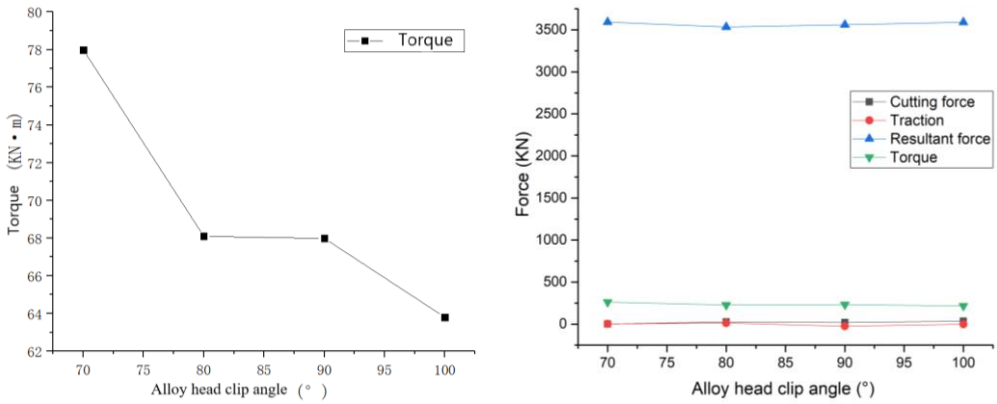


Fig. 8. The calculation results

According to Fig. 8 and Table 3, when the alloy head clip angle of the pick is 70°, the cutting force is the minimum, which is 2.41 kN. With the increase of the alloy head clip angle, the cutting force of the cutting head increases first and then decreases and increases again. When the alloy head clip angle is 100°, the cutting force reaches the maximum and the wear is the most serious. When the alloy head clip angle is between 70° and 80°, the difference between the simulation results of cutting force is about 24.13 kN, that is, 91%, compared with the simulation results of the alloy head clip angle of 70°, the change is great. When the included the alloy head clip angle is between 80° and 100°, the simulation results of cutting force difference are 16.25 kN. The resultant force fluctuation range of the included angle of the four alloy heads is not large, the maximum difference is 58.67 kN, that is, the variation range is 1.6%.

It can also be seen from Fig. 8 and Table 3 that the standard deviation of the resultant force is between 70° and 100°, decreases first, then increases and then decreases, and reaches the minimum value when the included alloy head clip angle is 80°. The fluctuation range of standard deviation of the resultant force is 34.11 kN, that is, the variation range is 13%.

Specific energy consumption H_w represents the energy consumed by cutting per unit volume (Zhao et al. 2014):

$$H_w = \frac{\rho_m t n T_M}{9550 \times 3600 M_m}, \tag{7}$$

where: H_w is specific energy consumption, kW·h/m³, ρ_m is rock density, m³, t is the time, s, n is rotation speed, r/min, T_m is torque, N·m; M_n is rock shedding mass, kg.

Table 4. Cutting specific energy consumption

Alloy head clip angle [°]	Torque [KN*m]	Speed [r/min]	Time [s]	Falling mass of rock [kg]	Specific energy consumption [kW·h/m ³]
70	77.99	38	1	115.61	1.38
80	68.09	38	1	118.56	1.17
90	67.98	38	1	115.25	1.20
100	63.80	38	1	114.87	1.14

According to the data in Table 4, the relationship between the included the alloy head clip angle and the specific energy consumption of the cutting head can be obtained, as shown in Fig. 9 below.

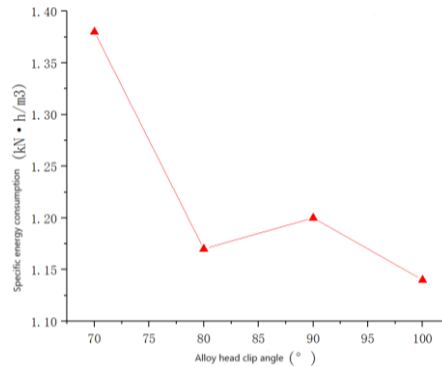


Fig. 9. Cutting specific energy consumption

As can be seen from Fig. 9, cutting specific energy consumption decreases first, then increases, and then decreases with the increase of alloy head diameter. The range of cutting specific energy consumption is 0.16 kW·h/m³, about 11.1%. When the alloy head diameter is 16mm, the specific energy consumption of cutting head is the minimum, which is 1.27 kW·h/m³, which can be used as an important index of energy evaluation.

3.2. THE ALLOY HEAD DIAMETER

Through calculation, the torque and other data of cutting head with different alloy head clip angles when crushing rock can be obtained, as shown in Table 5.

Table 5. The calculation results

Alloy head diameter [mm]	Torque [KN*m]	Speed [r/min]	Time [s]	Falling mass of rock [kg]	Specific energy consumption [kW·h/m ³]
--------------------------	---------------	---------------	----------	---------------------------	--

9	78.89	38	1	115.61	1.38
11	72.39	38	1	118.56	1.17
13	74.57	38	1	115.25	1.20
16	74.80	38	1	114.87	1.14

According to the data in Table 5, draw the relationship between the included the alloy head clip angle and the specific energy consumption of the cutting head, as shown in Fig. 10 below.

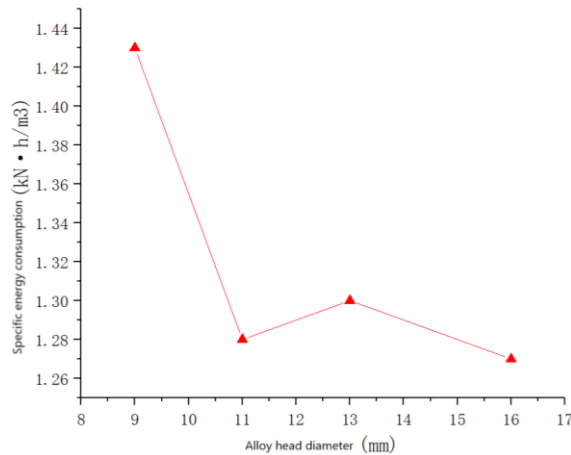


Fig. 10. Cutting specific energy consumption

As can be seen from Fig. 10, cutting specific energy consumption decreases first, then increases, and then decreases with the increase of the alloy head diameter. The range of cutting specific energy consumption is $0.16\text{kW}\cdot\text{h}/\text{m}^3$, about 11.1%. When the alloy head diameter is 16mm, the unit energy consumption of the cutting head is the minimum, which is $1.27\text{ kW}\cdot\text{h}/\text{m}^3$, which can be used as an important index of energy evaluation.

3.3. CALCULATION BASED ON THE FUZZY NUMBER AND ENTROPY EVALUATION METHOD

3.3.1. DETERMINATION OF INDEX SET AND EVALUATION SET OF CUTTING HEAD

1. Establish a cutting head index set

This paper mainly studies the load fluctuation, the load of the cutting head, the torque and the specific energy consumption, among which, the load fluctuation can be expressed by the standard deviation of the resultant force (Gogoi, Chutia 2022).

Therefore, the set of established evaluation indicators is:

$U = \{u_1, u_2, u_3, u_4\} = \{\text{The load of the cutting head, The load fluctuation, The torque, The specific energy consumption}\}$

2. Establish an evaluation set

In this paper, the performance parameters of the pick can be divided into three grades: excellent, good, and average (Kumar, Kumar 2021).

Therefore, the set of established evaluation indicators is:

$$V = \{v_1, v_2, v_3\} = \{\text{Excellent, Good, Average}\}$$

3.3.2. DETERMINE THE WEIGHT VECTOR OF CUTTING HEAD EVALUATION INDEX

Set n samples and m indicators to establish the sample matrix

$$S = \begin{bmatrix} S_{11} & \cdots & S_{1n} \\ S_{21} & \cdots & S_{2n} \\ \vdots & \ddots & \vdots \\ S_{m1} & \cdots & S_{mn} \end{bmatrix}, \quad (9)$$

where the actual value of S_{ij} sample i regarding indicator j .

1) Dimensionless treatment, extreme value method is used to calculate the formula as follows.

For the index that the greater is the better, there is the following formula:

$$X_{ij} = \frac{S_{ij} - \min_j(S_{ij})}{\max_j(S_{ij}) - \min_j(S_{ij})}. \quad (10)$$

For the smaller is better index, there is the following formula:

$$x_{ij} = \frac{\max_j(S_{ij}) - (S_{ij})}{\max_j(S_{ij}) - \min_j(S_{ij})}. \quad (11)$$

2) Calculating the weight y_{ij} of the i -th object index value of the j -th index.

$$y_{ij} = \frac{x_{ij}}{\sum_{i=1}^n x_{ij}}. \quad (12)$$

3) Calculating the entropy of the j -th index.

$$e_j = -\frac{1}{\ln n} \sum_{i=1}^n \ln y_{ij}, \quad (13)$$

where n is the number of samples.

4) Calculate coefficient of difference

$$d_j = 1 - e_j \tag{14}$$

5) Determining the weight of evaluation index w_j .

$$w_j = \frac{d_j}{\sum_{j=1}^n d_j} \tag{15}$$

3.3.3. DETERMINING MEMBERSHIP FUNCTION

Membership function is a quantitative description of the fuzzy number M, and the main membership function includes matrix, trapezoid, parabolic, normal and Cauchy type, etc. (Kumar, Gajpal 2021). In this paper, triangle type is adopted, and its formula is as follows.

$$r_{ij} = \begin{cases} 0 & x < x_i \\ \frac{x - x_i}{b - x_i} & x_i \leq x \leq b \\ \frac{x_{i+1} - x}{x_{i+1} - b} & b \leq x \leq x_{i+1} \\ 0 & x \geq x_{i+1} \end{cases}, \tag{16}$$

$$b = -\frac{1}{2}(x_i + x_{i+1}), \tag{17}$$

where: x is the actual value, x_i and x_{i+1} are upper and lower bounds of x .

3.3.4. ESTABLISHING FUZZY RELATION MATRIX

Through Eqs. (16) and (17), the fuzzy relation matrix R composed of R_{ij} can be obtained, and the established fuzzy relation matrix R is:

$$R = \begin{bmatrix} r_{11} & r_{12} & \cdots & r_{1n} \\ r_{21} & r_{22} & \cdots & r_{2n} \\ \vdots & \vdots & \ddots & \vdots \\ r_{m1} & r_{m2} & \cdots & r_{mn} \end{bmatrix}, \tag{18}$$

where R_{ij} is the membership degree of single index to the j -th comment.

3.3.5. COMPREHENSIVE EVALUATION CALCULATION

After fuzzy operation and processing of the obtained fuzzy relation matrix R and the weight vector S of the evaluation index, the fuzzy comprehensive evaluation model can be obtained as shown in formula (19).

$$B = S \cdot R = (w_1, \dots, w_n) \cdot \begin{bmatrix} r_{11} & r_{12} & \cdots & r_{1n} \\ r_{21} & r_{22} & \cdots & r_{2n} \\ \vdots & \vdots & \ddots & \vdots \\ r_{m1} & r_{m2} & \cdots & r_{mn} \end{bmatrix}. \quad (19)$$

The result vector of fuzzy comprehensive evaluation is obtained.

$$B = (b_1, b_2, b_m). \quad (20)$$

So, the expected value of B is $E(B)$.

$$E(B) = b_1 + 2b_2 + b_3 / 4. \quad (21)$$

3.3.6. THE CALCULATION RESULTS

Since the energy consumption and economic benefit need to be considered in the actual work, the pick performance parameters with the highest specific energy consumption in each set of simulation results are removed in the evaluation of design results (Kané et al. 2014).

Taking the included angles of different alloy heads as an example, after removing the performance parameters of the pick with the highest energy consumption, the performance parameters are shown in Table 6.

Table 6. The calculation results

Alloy head clip angle [°]	Cutting force [KN]	The standard deviation of the resultant force	Torque [KN*m]	Specific energy consumption [kW-h/m ³]
80	26.54	227.22	68.09	1.17
90	20.64	233.43	67.98	1.20
100	36.89	228.36	63.80	1.14

After fuzzy number processing, the fuzzy values of motion parameters obtained are shown in Table 7.

Table 7. The calculation results

Alloy head clip angle [°]	80°	90°	100°
Cutting force [KN]	(1, 2, 3)	(2, 3, 4)	(1, 1, 2)
The standard deviation of the resultant force	(2, 3, 4)	(1, 1, 2)	(1, 2, 3)
Torque [KN*m]	(1, 1, 2)	(1, 2, 3)	(2, 3, 4)
Specific energy consumption [kW·h/m ³]	(1, 2, 3)	(1, 1, 2)	(2, 3, 4)

By using formulas (9), (11)–(15), the weight of different pick motion parameters is:

$$W_1 = \{0.1883, 0.1797, 0.4297, 0.2022\}.$$

According to Table 7 and formula (19), the fuzzy evaluation vector of comprehensive performance of different alloy head angles can be obtained as follows:

$$B_1 = (1.18, 1.75, 2.75), \tag{22}$$

$$B_2 = (1.19, 1.81, 2.81), \tag{23}$$

$$B_3 = (1.63, 2.44, 3.44). \tag{24}$$

The expected values of each fuzzy evaluation vector can be obtained from Eq. (21)

$$E(B_1) = 1.86,$$

$$E(B_2) = 1.91,$$

$$E(B_3) = 2.49.$$

Because of $E(B_1) < E(B_2) < E(B_3)$, so the optimal included the alloy head clip angle is 100°. At this time, the overall performance is also optimal.

Similarly, the fuzzy evaluation vectors and expected values of the comprehensive properties of different alloy head diameters can be calculated.

The fuzzy evaluation vector of comprehensive performance of different alloy head diameters is:

$$B_1 = (1.64, 2.46, 3.46), \tag{25}$$

$$B_2 = (1.18, 1.71, 2.71), \tag{27}$$

$$B_3 = (1.19, 1.84, 2.84), \tag{28}$$

The expected value can be obtained from Eq. (21).

$$E(B_1) = 2.51,$$

$$E(B_2) = 1.83,$$

$$E(B_3) = 1.93.$$

The optimum the alloy head diameter is 11 mm.

4. CONCLUSION

By using fuzzy number principle and entropy evaluation method, the fuzzy evaluation vector of weight and comprehensive performance is obtained by using comprehensive evaluation method. Using the principle of maximum membership degree, the optimal value of each sample was selected, and the optimal performance parameters were obtained as follows: the alloy head clip angle 100° , the alloy head diameter 11 mm.

ACKNOWLEDGEMENTS

This study was financially supported by the National Natural Science Foundation of China (52105243), the Hunan Provincial Natural Science Foundation of China (2020JJ4646), the Research Foundation of Education Bureau of Hunan Province, China (19C0168).

REFERENCES

- SU O., AKKAŞ M., 2020, *Assessment of pick wear based on the field performance of two transverse type roadheaders: a case study from Amasra coalfield*, Bulletin of Engineering Geology and the Environment, 79(5), 2499–2512.
- ESHAGHIAN O., HOSEINIE S.H., MALEKI A., 2021, *Multi-attribute failure analysis of coal cutting picks on longwall shearer machine*, Engineering Failure Analysis, 120, 105069.
- QIAO S., ZHANG Z.Q., ZHU Z.M. et al., 2021, *Influence of cutting angle on mechanical properties of rock cutting by conical pick based on finite element analysis*, Mining Science, 28.
- YIXUE L., 2019, *Mechanical Analysis of Cutting Head Based on ANSYS Tunneling Machine on ANSYS Tunneling Machine*, Taiyuan University of Science and Technology, DOI: 10.27721/d.cnki.gyzjc.2019.000315.
- QIAN W., 2020, *Study on the Mapping Relationship Between Vibration of Cutting Head of Rock Roadheader and Rock Hardness*, Taiyuan University of Technology, DOI:10.27352/d.cnki.gylgu.2020.000483.
- HEKIMOGLU O.Z., 2018, *Investigations into tilt angles and order of cutting sequences for cutting head design of roadheaders*, Tunnelling and Underground Space Technology Incorporating Trenchless Technology Research, 76, 160–171.
- HOLMQUIST T.J., JOHNSON G.R., COOK W.H., 1993, *A computational constitutive for concrete subjected to large strains, high strain rates and high pressure*, Proceeding of the Fourteenth International Symposium on Interactics, 2, 591–600.
- XVTAO WU, YAO LI, HEPING LI, 2010. *Research on the material constants of the H-J-C dynamic constitutive model for concrete*, Chinese Journal of Applied Mechanics, 27(02), 340–344, 443.

- WEILING SU, XINGGAO LI, YU XU, DALONG JING, 2020, *Numerical simulation of shield tool cutting concrete based on H-J-C model*, Journal of Zhejiang University (Engineering Science), 54(06), 1106–1114.
- YAO LI, 2009, *Research on H-J-C dynamic constitutive model for concrete*, Hefei University of Technology.
- SHUO QIAO et al., 2022, *Modelling and experimental investigation of cobalt-Rich crust cutting in ocean environment*, Ocean Engineering, 245 (2022), 110511.
- SHUO QIAO et al., 2021, *Numerical Investigation of Rock Cutting Modes with Conical Picks under Different Confining Pressures and Cutting Spaces*, Arabian Journal for Science and Engineering, (2021), 1–11.
- SHUO QIAO et al., 2021, *Research on cobalt-rich crust cutting modes by deep-sea mining vehicle and cutting performance evaluation*, Marine Georesources and Geotechnology, (2021), 1–8.
- LIYING ZHANG, MENGQI ZHANG, 2020, *Simulation on load of cutting head whose picks in cross-type arrangement with various spiral lines*, Mining and Processing Equipment, 48, 10 (2020), 1–8. DOI: 10.16816/j.cnki.ksjx.2020.10.001.
- STOLARSKI T., NAKASONE Y., YOSHIMOTO S., 2018, *Engineering analysis with ANSYS software*, Butterworth-Heinemann.
- LIJUAN ZHAO et al., 2014, *Influence of pick arrangement mode on shearer's working performance*, Mechanical Science and Technology for Aerospace Engineering, 33(12), 1838–1844.
- GOGOI MRIDUL KRISHNA, CHUTIA RITUPARNA, 2022, *Fuzzy risk analysis based on a similarity measure of fuzzy numbers and its application in crop selection*, Engineering Applications of Artificial Intelligence, 107(2022), DOI: 10.1016/J.ENGAPPAL.2021.104517.
- KUMAR SANDEEP, KUMAR MOHIT, 2021, *A New Approach to Solve Group Decision Making Problems with Attribute Values and Attribute Weights Represented by Interval-Valued Intuitionistic Fuzzy Numbers*, International Journal of Applied and Computational Mathematics 7.4(2021), DOI: 10.1007/S40819-021-01101-7.
- APPADOO S., Kumar A., GAJPAL Y., 2021, *Generalized exponential trapezoidal fuzzy numbers based on variance*, Journal of Information and Optimization Sciences 42.7(2021). DOI: 10.1080/02522667.2021.1877403.
- KANÉ LADJI et al., 2021, *A Mathematical Model for Solving the Linear Programming Problems Involving Trapezoidal Fuzzy Numbers via Interval Linear Programming Problems*, Journal of Mathematics, (2021), DOI: 10.1155/2021/5564598.